Identification of the mechanism of NO reduction with ammonia (SCR) on zeolite catalysts

Konstantin Khivantsev[1*]†, Ja-Hun Kwak[2*]†, Nicholas R. Jaegers[1*], Iskra Z. Koleva[3]†, Georgi N. Vayssilov[3], Miroslaw A. Derewinski[1,4], Yong Wang[1], Hristiyan A. Aleksandrov[3*]† and Janos Szanyi[1*]†

[1]Pacific Northwest National Laboratory Richland, WA 99352 USA

[2] Ulsan National Institute of Science and Technology (UNIST), South Korea

[3]Faculty of Chemistry and Pharmacy, University of Sofia, 1126 Sofia, Bulgaria

[4] J. Haber Institute of Catalysis and Surface Chemistry, Polish Academy of Sciences, Krakow 30-239, Poland

*corresponding authors: KK, J-H. Kw., NRJ, HAA, J. Sz.

†these authors contributed equally

Cu/Zeolites efficiently catalyze selective reduction of environmentally harmful nitric oxide with ammonia. Despite over a decade of research, the exact NO reduction steps remain unknown. Herein, using combined spectroscopic, catalytic and DFT approach we show that nitrosyl ions (NO^+) in the zeolitic micropores are the key intermediates for NO reduction. Remarkably, they react with ammonia even below room temperature producing molecular nitrogen (the reaction central to turning NO pollutant to benign nitrogen) through the intermediacy of the diazo N_2H^+ cation. Experiments with isotopically labeled N-compounds confirm our proposed reaction path. No copper is required for N_2 formation to occur during this step. However, at temperatures below 100 ºC, when NO^+ reacts with NH_3, the bare Brønsted acid site becomes occupied by NH_3 to form strongly bound NH_4^+ and, consequently, this stops the catalytic cycle, because NO^+ cannot form on NH_4-Zeolites when their H^+ sites are already occupied by NH_4^+. On the other hand, we show the reaction becomes catalytic on H-zeolites at temperatures when some ammonia desorption can occur (>120 ºC). We suggest that the role of Cu(II) ions in Cu/Zeolite catalysts for low-temperature NO reduction is to produce abundant NO^+ by the reaction: Cu(II) + NO → Cu(I)---NO^+. NO^+ then reacts with ammonia to produce nitrogen and water. Furthermore, when Cu(I) gets re-oxidized the catalytic cycle then can continue. Our findings provide novel understanding of the hirtherto unknown steps of the SCR mechanism pertinent to N-N coupling. The observed chemistry of Cu ions in zeolites bears striking resemblance to the copper-containing denitrification and annamox enzymes, which catalyze transformation of NO_x species to N_2, via di-azo compounds.

Air pollution is one of the main health and environmental concerns in our (post)industrial society [1-3]. Worsened air quality during industrial expansion is attributed to a great extent to toxic nitric oxide (NO) gas, where nearly 55% of the global emissions are due to transportation exhaust. The ability of Cu/zeolites to turn NO to N_2 in the presence of ammonia was first discovered in Japan in the 1960s [4] for Cu/FAU zeolite. However, the FAU framework is less stable than the corresponding SSZ-13 and BEA zeolites [5]. Within the last decade, the ammonia selective catalytic reduction (SCR) technology was implemented on the large scale [5-19] for diesel engines on the basis of Cu(Fe) in BEA and SSZ-13 zeolites.

Some advances were achieved towards the goal of understanding the rate-limiting steps of the SCR mechanism [5-20]. Cu(II) ions are present in Cu/zeolite materials as well as Cu(II)-OH ions [5-20,25]. The rate-limiting step for low-temperature SCR, for low copper loaded materials (Cu loading below 0.5 wt%), was shown to be the re-oxidation of reduced $Cu(I)(NH_3)_2$ complexes via the formation of transient $(NH_3)_2Cu(II)\text{-}O_2\text{-}Cu(II)(NH_3)_2$ dimers [17,18]. However, the steps involved in the exact mechanism of NO reduction to N_2 have remained unknown [5-20] and the proposed DFT steps were shown hard to prove/observe experimentally.

In this study we selectively formed NO^+ ions in H-BEA zeolite (typical helium ion microscopy images of H-BEA are shown in Figure S0) by reaction of NO with O_2 (Figure 1A).[21-23] NO^+ is formed through the reaction depicted in **Scheme 1:**

Scheme 1:

$2NO + 1/2O_2 + 2$ H-Zeolite → $2NO^+ + H_2O + 2$ Zeolite$^-$

NO^+ occupies two different cationic positions with the corresponding N-O stretching frequencies at ~2133 and ~2175 cm^{-1}. The same type of chemistry also occurs on H-SSZ-13 (Figure S1). Note that adsorption of NO_2 also produces NO^+ but with stoichiometric NO_3^- amounts due to N_2O_4 disproportionation (Figure S2). Our DFT calculations further corroborate the described chemistry *vide infra*.

Evacuation to high vacuum (~10^{-7} Torr) (with quick heating to 150 ºC) allows the removal of excessive NO and O_2, leaving the zeolite with NO^+ adsorbed in it (Figure 1B).

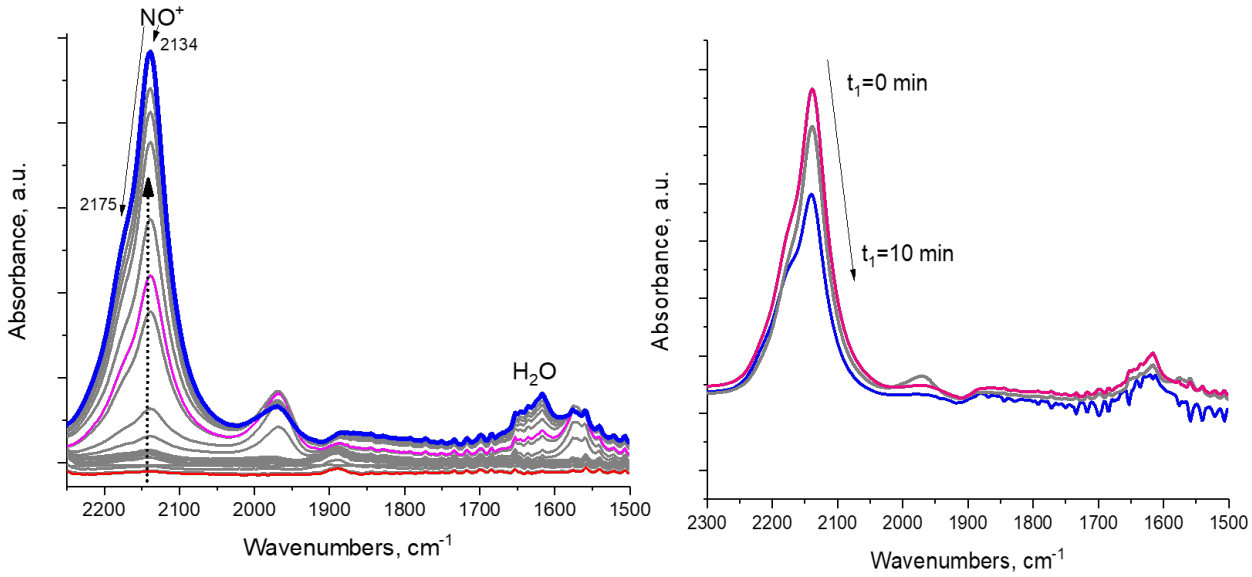

Figure1. H-BEA Zeolite with Si/Al ~ 15. **A (left spectrum)**: *in-situ* FTIR during first sequential NO adsorption (0.1 Torr equilibrium pressure), followed by sequential O_2 addition (0.17 Torr total eq. pressure – when O_2 is added, NO^+ begins to develop in significant amounts); T=20 ºC **B (right spectrum)**: FTIR spectra collected after pulling high vacuum 10^{-8} Torr from time=0 to time=10 minutes at 150 ºC. Spectra were recorded after cooling back to 20 ºC.

We exposed the NO^+/Zeolite to ^{15}N-labeled ammonia at room temperature (~20 ºC) (Figure 2A). Ammonia first occupies Brønsted acid sites forming NH_4^+ complexes which interact with NH_3 in the pores, generating $(NH_3)x$ cluster networks interacting with NH_4^+ ions [24,27]. During this, NO^+ reacts with ammonia, as evidenced by the swiftly diminishing NO^+ band, eventually leaving no new visible NO stretches as the excess of $^{15}NH_3$ produces the complex bands typical for NH_4^+-$(NH_3)_x$ clusters in zeolites in the 2250-1750 cm^{-1} region [25] (Figure 2A).

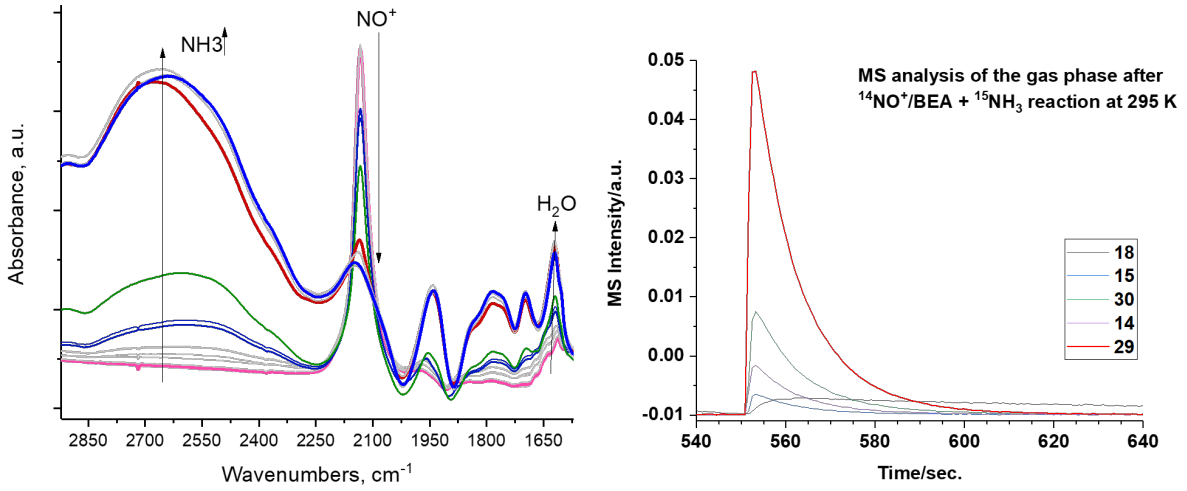

Figure 2. H-BEA zeolite with Si/Al~15. **A (left spectrum)**: *in-situ* sequential FTIR during $^{15}NH_3$ adsorption (total equilibrium pressure 0.020 Torr) on NO^+/H-BEA sample at 20 ºC. Ammonia reacts with NO^+. The gas phase effluent from the reaction (T!20 ºC) was analyzed with the mass spectrometer attached to the IR cell. **Figure 2B** shows formation of $^{14}N^{15}N$ dinitrogen with the characteristic m/z = 29 signal.

The analysis of the gas-phase product with mass-spectrometry reveals a major peak at 29 amu per charge, corresponding to ^{14}N-^{15}N molecules (Figure 2B). Thus, NO^+ reacts with ammonia to form molecular nitrogen at room temperature on H-BEA. **Schemes 2 and 3** can be envisioned to describe this process. Note that NO^+ does not necessarily have to be bound to zeolite in the presence of NH_3 and can initially become solvated by NH_3 (it is well-known that ammonia has propensity to solvate cationic species in and outside zeolites [17,18,25]; our DFT calculations in Table 1 further confirm strong favorability of NO^+ solvation by ammonia with energy gain of 95 kJ/mol); the designation Zeolite-NO^+ is just a representation of the NO^+/H-zeolite system in which NO^+ may be solvated or semi-solvated by ammonia molecules.

Scheme 2:

Zeolite-$N^{14}O^+ + N^{15}H_3$ → Zeolite-$N^{14}O(^{15}NH_3)$ → [Zeolite-$N^{14}(OH)N^{15}H_2$] → Zeolite-[$^{14/15}N_2H^+$] + H_2O

Scheme 3:

[Zeolite-$^{14/15}N_2H^+$] → Zeolite-H + N^{14}-N^{15}

The hydronium diazonium cation (N_2H^+) is extremely unstable. Its immediate decomposition to N_2 and H-Zeolite drives the reaction forward. Despite that, we find that at sufficiently high molecular N_2 pressure in the cell (~15Torr) we can observe the N-N stretch of the -HN_2^+ complex at 2,334 cm^{-1} even at room temperature (Figure 3A), which was previously shown to form at low temperatures upon N_2 interaction with Brønsted acid sites (Figure 3B) [26]. Thus, we can observe the intermediate of this reaction indirectly.

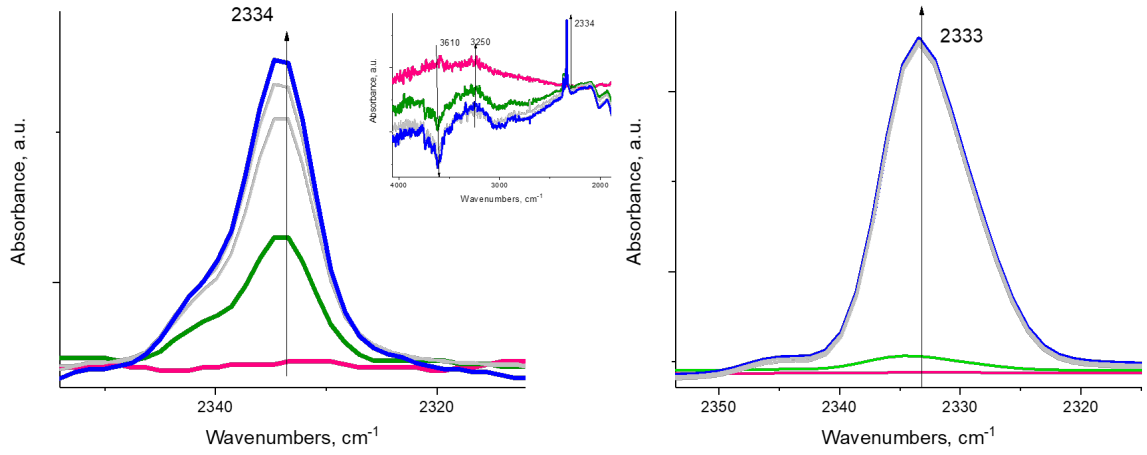

Figure 3. **A (left spectrum)**: *in-situ* FTIR during sequential dinitrogen N_2 adsorption (equilibrium pressure ~15 Torr) on H-BEA at ~23 ºC. Very unstable Zeolite-[HN_2^+] complex can be observed even at room temperature, but it requires elevated N_2 pressure. Inset shows that N_2 interacts with Brønsted acid sites of Si-OH-Al zeolite groups (OH stretch of such groups is located at ~3610 cm^{-1}). **B(right spectrum)**: *in-situ* FTIR during adsorption of only ~0.1 Torr N_2 on the same H-BEA sample (equilibrium pressure is 0.001 Torr) at 77 K produces N-N stretches of N_2 adsorbed on Brønsted acid sites. Note that in this case even low equilibrium pressure of nitrogen produces intense N-N stretches.

To further demonstrate that the reaction proceeds through a diazo compound, we chose aniline $PhNH_2$, an equivalent to the ammonia molecule but with 1 hydrogen atom substituted by a phenyl group and reacted it with NO^+ in BEA zeolite. The phenyl group stabilizes the formation of PhN_2^+ salts (phenyl diazonium salts) through the mesomeric effect, and unlike alkyl diazonium salts, aryl diazonium compounds are stable and characterized by N-N stretches in ~2,250-2,300 cm^{-1} region [28], more specifically

~2,270 cm^{-1} for phenyl diazonium in solution [28]. Indeed, we monitored the reaction of NO^+ and $PhNH_2$, spectroscopically: the intensity of the NO^+ band diminished and a new N-N stretch appeared at ~2,270 cm^{-1}, corresponding to the N-N vibration of the Ph-N_2^+ fragment (Figure 4).

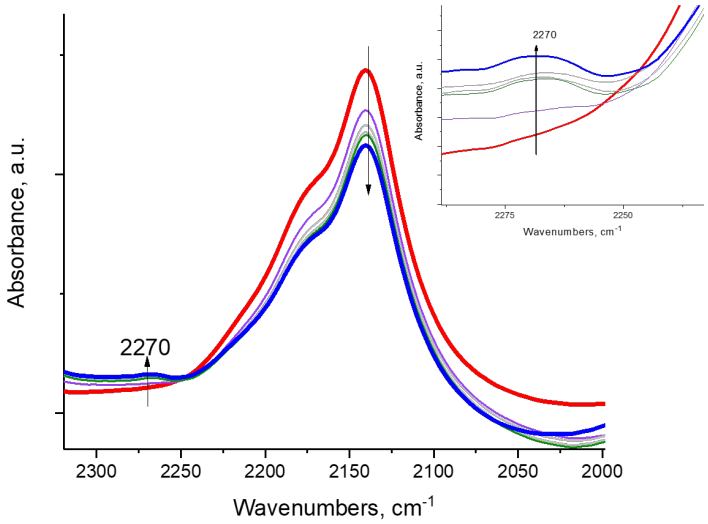

Figure 4. *in-situ* FTIR during sequential ~0.3 Torr aniline $PhNH_2$ adsorption (equilibrium pressure ~0.03 Torr) NO^+/H-BEA.

NO^+ in H-SSZ-13 (with Si/Al ~12; typical HAADF-STEM images of this sample are shown in Figure S7) reacts similarly with NH_3 (Figure 5), with concomitant N_2 evolution (confirmed with mass-spectrometry):

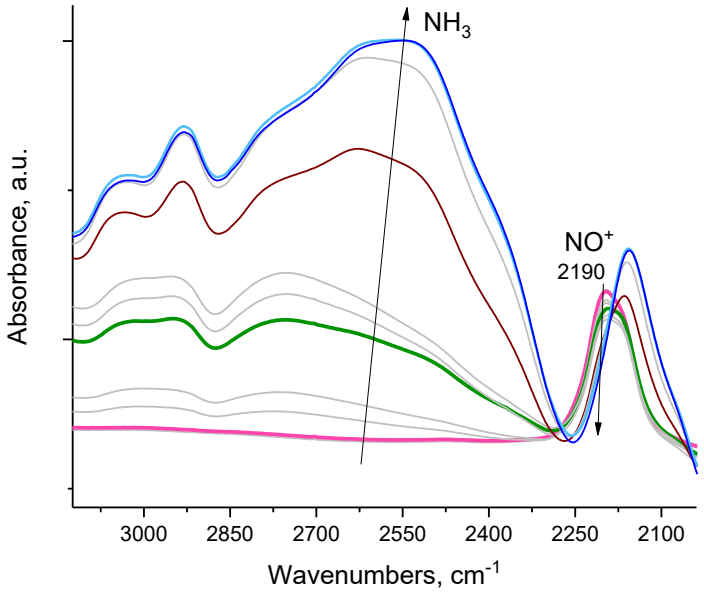

Figure 5. H-SSZ-13 zeolite with Si/Al~12. In-situ sequential FTIR during $^{14}NH_3$ adsorption (total equilibrium pressure ~0.15 Torr) on NO^+/H-SSZ-13 sample at 20 ºC. Ammonia reacts with NO^+ as evidenced by the disappearance of NO^+ stretch. The intense band at ~ 2,110 cm^{-1} is due to zeolite interactions with NH_3. Pulling vacuum on the sample at 120 ºC produces spectra showing no NO^+ stretches (Figure S3), consistent with complete reaction of NO^+.

As such, NO^+ is the critical intermediate species in the conversion of NO in these zeolites. Copper is not required to observe the NO^+ reactivity with NH_3. Moreover, we reacted inorganic nitrosyl salt NO^+ with $^{15}NH_3$ and observed ^{14}N-^{15}N in the gas-phase (consistent with our findings for NO^+ in zeolites, this reaction takes place vigorously even at temperatures as low -50 ºC) (**Scheme 4**):

Scheme 4:

$^{14}NO[BF_4] + {}^{15}NH_3$ (at -50 ºC)→ $^{14}N^{15}N$ (gas) + H_2O + $H[BF_4]$

This reaction (**scheme 4**) most likely proceeds through N_2H^+ intermediate as well.

For NO^+ in zeolite, once it reacts with NH_3 with the release of N_2, the Brønsted acid is free and immediately interacts with ammonia to produce NH_4^+. This latter process "kills" the reactivity as the NO^+ species can no longer be produced due to the necessity of Brønsted acid sites, as evidenced by FTIR (Figure S4): indeed, no NO^+ evolves above trace amounts upon NO+O_2 reaction on NH_4-zeolite (Figure S4). Only at elevated temperatures, when some NH_3 can desorb and free up a portion of Brønsted acid sites to re-form NO^+, can the reaction proceed catalytically which we show in Fig. S5. Bare H-BEA zeolite is catalytically active for NO reduction with NH_3 in the dry streams (see Figure S5 for reactivity at 200 and 150 ºC with time-on-stream) (measurable activity is observed). NO^+ are formed in zeolite through **Scheme 1** (see the earlier discussion in the manuscript).

With these new data, we can now further explain the possible role of Cu in zeolites for SCR. As is well-established in the literature, Cu(II) ions are required for the continuous catalytic reaction to proceed [5-20]. In the presence of NO, Cu(II) ions can produce NO^+ via 1-electron reduction of Cu(II) (analogous chemistry is observed, for example, for Pd(II) in zeolites [30] where Pd(II) was shown to reduce to Pd(I) by NO pulses with the concomitant formation of NO^+) (**Scheme 5**):

Scheme 5:

$Zeo_2Cu(II) + NO \rightarrow Zeo_1Cu(I)\text{---}NO^+\text{-}Zeo_1$

Figure 6A shows spectroscopic evidence of Cu(II) reduction by NO (when Cu(II) is first reduced to Cu(I) prior to NO adsorption, very little NO^+ formation occurs because electron transfer does not take place in the absence of Cu(II) as demonstrated in Figure 6B).

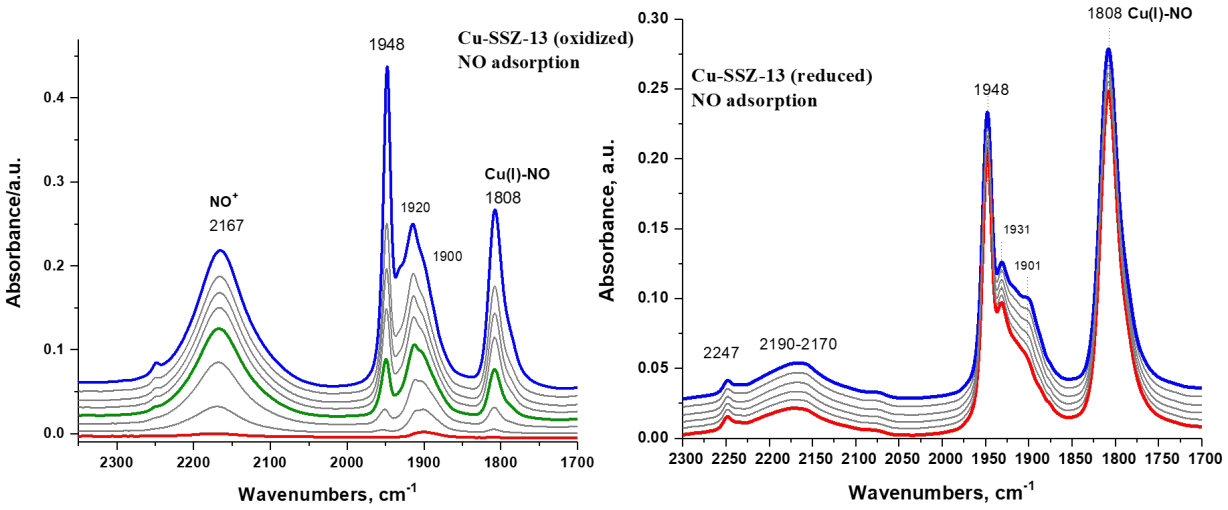

Figure 6. 1 wt% Cu/H-SSZ-13 sample with Si/Al ~ 12. **A (left)**: in-situ FTIR during 1 Torr NO adsorption on pre-oxidized sample (pre-oxidized in O_2 at 300 ºC). NO^+ and Cu(I)-NO evolve simultaneously from Cu(II) reduction by NO. **B (right)**: the same sample (tablet) was pre-reduced in the IR cell (at 300 ºC): 1 Torr NO adsorption (same equilibrium pressure) after reduction.

We have previously been able to confirm with solid-state ^{15}NMR studies that indeed NO is capable of reducing Cu(II) to Cu(I) in SSZ-13: the resulting complex had Cu(I) and NO^+ in proximity to each other, with NO^+ located side-on towards copper ion [20]. Similar chemistry is observed for Pd(II) in zeolite [30].

These novel experimental findings for NO^+ in zeolites prompted us to investigate the proposed reaction steps with density functional theory (DFT) calculations. First, we investigated two pathways for selective catalytic reduction of NO by the ammonia via formation of NO^+ species in the zeolite: (1) without (Figure 8, Table 1) and (2) with the direct (Figure 7, Table 1) participation of the zeolite. Both pathways start with adsorption of NH_3 to NO^+/Zeo with binding energy of ammonia of ~97 kJ/mol and subsequent formation

of nitrosamine via transfer of one of the H atoms from the ammonia to an O center from the AlO_4 tetrahedron.

A

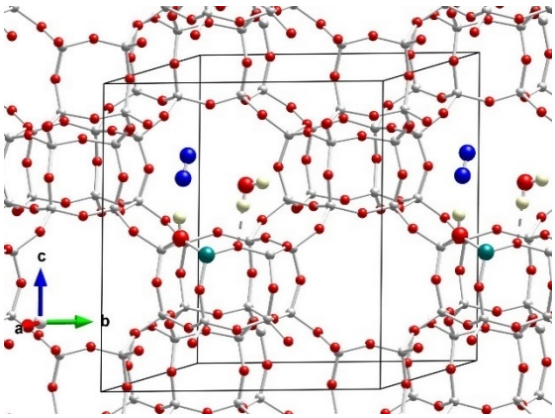

$(N_2 + H_2O)/H^+$-ZEO

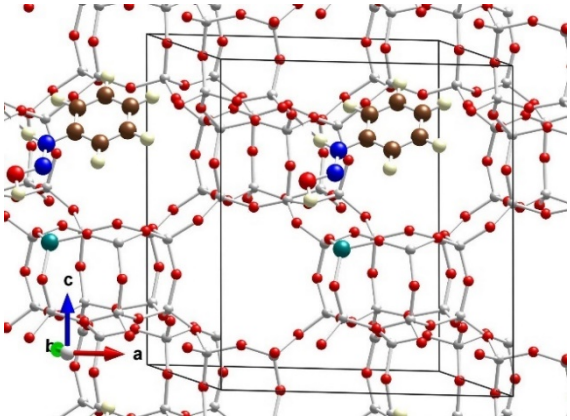

$PhNH{=}NOH^+$/ZEO

B

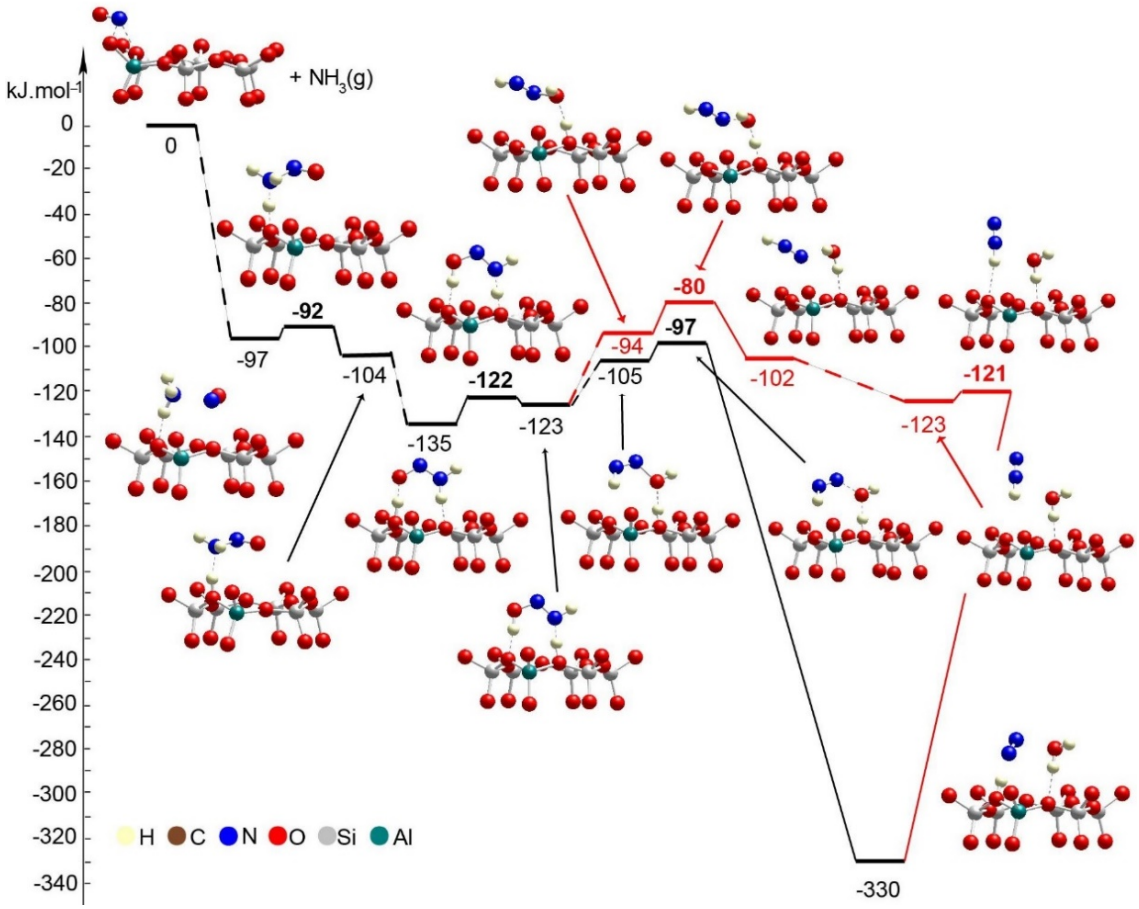

Figure 7. A. General location of the species in the pores of the unit cell of chabazite. Color coding: H – yellow; N – blue; C – brown; O – red; Al – green; Si – gray. **B.** Energy diagram and optimized models of reaction steps with the direct participation of the chabazite. Alternative reaction paths are shown in different colors. The models are visualized with VESTA program [34].

When the reaction step occurs via direct H transfer, the energy barrier is only 5 kJ/mol (Figure 7B, Table 1). We also found another transition state (TS) structure with elongated N-H distance (Figure 8, Table 1), it is less stable by more than 120 kJ/mol than the previous one. Further, one of the H atoms of NH_2 group of the nitrosamine should migrate to the O center of the same molecule thus forming HON=NH molecule. This can be done via H transfer occurring in the gas phase without the participation of the zeolite. In this case however, the reaction step is endothermic by 41 kJ/mol, while the barrier is as high as 148 kJ/mol. Alternatively, the process can occur stepwise with the direct participation of the zeolite support. In this case initially the molecule of nitrosamine reorientates so that two hydrogen bonds are formed between the guest molecule and support: N-H fragment with O center from zeolite and a zeolite proton with the O center from the nitrosamine. The new configuration is more stable by 31 kJ/mol than the previous one.

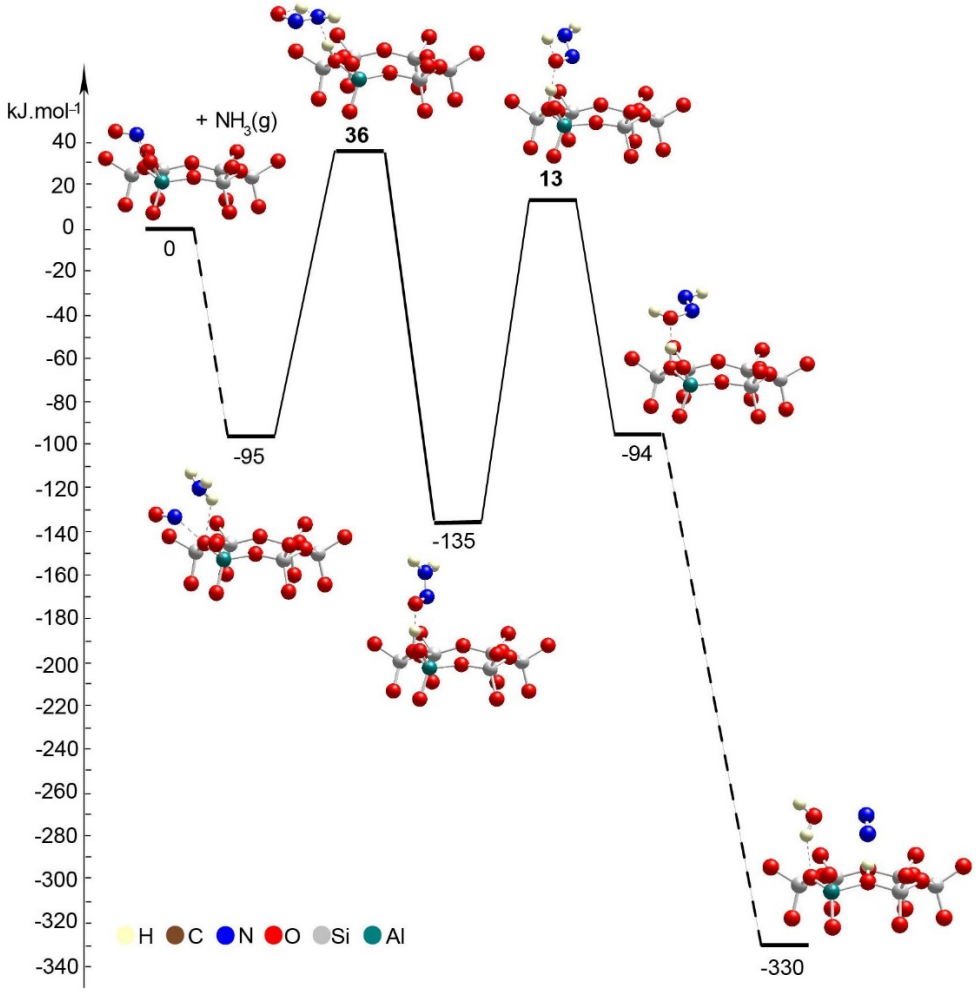

Figure 8. Energy diagram and optimized models of reaction steps with no direct participation of the chabazite. The models are visualized with VESTA program [34].

Table 1. Energies, ΔE, and activation barriers, E_a, of the modelled reaction steps.

Reaction	ΔE, kJ/mol	E_a, kJ/mol
Direct participation of the chabazite		
NO^+/ZEO + NH_3(g) → $NO^+(NH_3)$/ZEO	-97	–
$NO^+(NH_3)$/ZEO → $NONH_2/H^+$-ZEO	-7	5
$NONH_2/H^+$-ZEO → $NONH_2$_rotated1/H^+-ZEO	-31	–
$NONH_2$_rotated1/H^+-ZEO → HN=NOH/H^+-ZEO	12	13
HN=NOH/H^+-ZEO → HN=NOH_rotated1/H^+-ZEO	18	–
HN=NOH_rotated1 → (N_2 + H_2O)/H^+-ZEO	-225	8
HN=NOH/H^+-ZEO → HN=NOH_rotated2/H^+-ZEO [a]	29	–
HN=NOH_rotated2/H^+-ZEO → (NNH^+ + H_2O)/ZEO [a]	-8	14
(NNH^+ + H_2O)/ZEO → (NNH^+_rotated + H_2O)/ZEO [a]	-21	–
(NNH + H_2O)/ZEO → (N_2 + H_2O)/H^+-ZEO [a]	-207	2
No direct participation of the chabazite		
NO^+/ZEO + NH_3→ $NO^+(NH_3)$/ZEO	-95	
$NO^+(NH_3)$/ZEO → $NONH_2$_rotated3/H^+-ZEO	-40	131
$NONH_2$_rotated3/H^+-ZEO → HN=NOH_rotated3/H^+-ZEO	41	148
HNNOH_rotated3/H^+-ZEO → (N_2 + H_2O)/H^+-ZEO	-236	–
$PhNH_2$ transformation in the pores of ZEO/NO^+		
NO^+/ZEO + $PhNH_2$(g) → ($PhNH_2$-NO^+)/ZEO	-186	–
($PhNH_2$-NO^+)/ZEO → PhNH=NO/H^+-ZEO	5	31
PhNH=NO/H^+-ZEO → PhNH=NOH^+/ZEO	-49	3
PhNH=NOH^+/ZEO → PhN=NOH/H^+-ZEO	57	65
PhN=NOH/H^+-ZEO → (PhN=N^+ + H_2O)/ZEO	-69	11
(PhN=N^+ + H_2O)/ZEO → PhN=N^+/ZEO + H_2O(g)	26	–
PhNH=NOH^+/ZEO → PhN=N^+ + H_2O/ZEO [b]	-12	158
PhNH=NO/H^+-ZEO → PhN=NOH_rotated/H^+-ZEO [c]	-4	1
PhN=NOH_rotated/H^+-ZEO → (PhN=N^+ + H_2O)/ZEO [c]	-57	23
Interaction of BF_4/NO^+ with NH_3		
NO^+/BF_4^- + NH_3(g) → $NO^+(NH_3)$	-91	–
$NO^+(NH_3)/BF_4^-$ → $NONH_2/BF_3$-HF	15	16
$NONH_2/BF_3$-HF → $NONH_2$_rotated1/BF_3-HF	-42	–
$NONH_2$_rotated1/BF_3-HF → HN=NOH/BF_3-HF	-3	2
HN=NOH/BF_3-HF → HN=NOH_rotated1/BF_3-HF	31	–
HN=NOH/BF_3-HF_rotated1 → (N_2 + H_2O)/BF_3-HF	-221	1
HN=NOH/BF_3-HF → HN=NOH_rotated2/BF_3-HF [d]	44	–
HN=NOH_rotated2/BF_3-HF → (NNH^+ + H_2O)/BF_4^- [d]	-17	16
$NONH_2/BF_3$-HF → $NONH_2$_rotated2/BF_3-HF [e]	-25	–
$NONH_2$_rotated2/BF_3-HF → HN=NOH_rotated3/BF_3-HF [e]	17	126

Alternative reaction paths: [a] marked in red color on Fig. 7B; [b] marked in red color on Fig. 9; [c] marked in blue color on Fig. 9; [d] marked in red color on Fig. 10; [e] marked in blue color on Fig. 10.

Further, via synchronous transition state structure the H atom from the NH fragment moves to the zeolite O center and simultaneously the zeolite proton migrates to the O atom from the guest molecule. The

energy barrier is only 13 kJ/mol, while the reaction step is only slightly endothermic by 12 kJ/mol. In the next step the HON=NH molecule should be converted into the final products: H_2O and N_2. This can be done again via direct H transfer in the gas phase from the N to the O atom with no direct participation of the zeolite support. Based on the previous knowledge it is expected that reaction step will have high barrier. Alternatively, we considered the process with the participation of the zeolite, as two reaction pathways were considered: concerted and stepwise pathways, as in both cases initially the guest molecule changes its position with respect to the zeolite support as one of the hydrogen bonds, NH---O, breaks. The new structures are less stable by 18 and 29 kJ/mol than the final state structure of the previous reaction step. In the concerted mechanism in one step the zeolite proton moves to the OH group from the HON=NH species, thus forming a water molecule, while the H bound to the N atom moves to an O zeolite center forming a N_2 molecule. The reaction step is strongly exothermic, -225 kJ/mol, with very low barrier, 8 kJ/mol. Alternatively, in the stepwise mechanism first H_2O and NNH^+ can be formed overcoming a low barrier of 14 kJ/mol as the reaction step is slightly exothermic, -8 kJ/mol. Next NNH^+ reorients so that a hydrogen bond is formed with zeolite O center. In the final step H moves to the zeolite O center, this bridging OH group and N_2 molecule are formed. This step is essentially barrierless and strongly exothermic, -207 kJ/mol. These DFT results confirm favorability of NO^+ interaction with NH_3 to form N_2 basically with little to no barriers, consistent with the experimentally observed low-temperature reactivity of these species.

Next, we modeled the reduction process using aniline $PhNH_2$ interacting with NO^+ species positioned as charge-compensating cation in chabazite (Figure 9, Table 1).

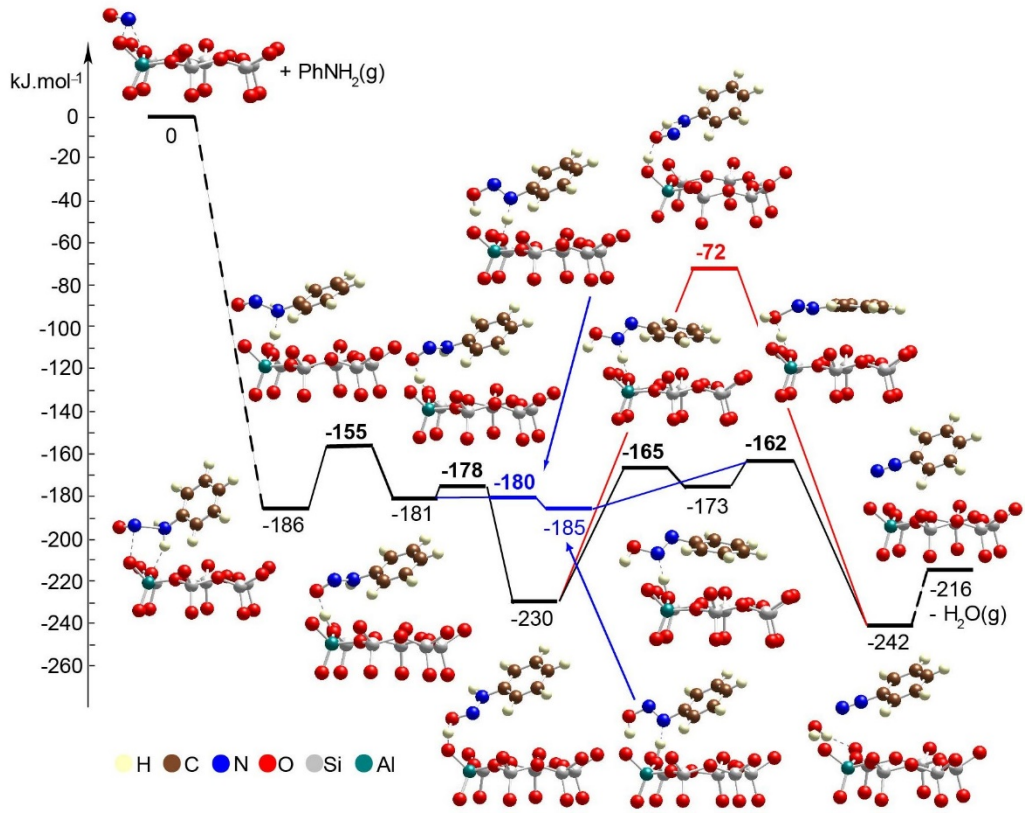

Figure 9. Energy diagram and optimized models of the reaction steps for the $PhNH_2$ transformation in the pores of ZEO/NO^+. The models are visualized with VESTA program [34].

The adsorption energy of aniline to NO^+ species is -186 kJ/mol. Further, one of the H atoms of the amino groups migrates to the O center from the zeolite, thus forming ONNHPh coordinated to the zeolite proton. This reaction step is slightly endothermic by 5 kJ/mol and its energy barrier is 31 kJ/mol. From the latter structure one can obtain benzenediazonium cation, $PhNN^+$, via two alternative pathways:

- In the more plausible pathway HONNPh structure is formed via synchronous TS structure in which zeolite proton migrates on the O atom from the organic molecule, while the H atom from NH fragment moves to a zeolite O center. The reaction step is essentially barrierless and very slightly exothermic, -4 kJ/mol. Further, the zeolite proton interacts with the OH group from the organic molecule which leads to formation of $PhNN^+$ and water molecule. The barrier for this reaction step is 23 kJ/mol and it is exothermic by 57 kJ/mol.

- The alternative pathway requires overcoming of higher barriers than in the first one. In the first step the zeolite proton migrates to the O center from the organic molecule as $PhNH{=}NOH^+$ is formed. The process is essentially barrierless and exothermic by 49 kJ/mol. At the final stage $PhNN^+$ cation should be formed, as we considered two possible reaction pathways. In the concerted mechanism in one step the O center

forms bonds with both H centers which are initial positioned at zeolite O center and N atom from the organic molecule. The second H transfer is in the gas phase without direct participation of the zeolite which leads to unstable transition state structure, thus the barrier is 158 kJ/mol and reaction energy is only slightly exothermic by 12 kJ/mol. In the stepwise mechanism H atom bound to the N center is transferred to an O zeolite center forming HON=NPh molecule. This reaction step is endothermic by 57 kJ/mol and the barrier is 65 kJ/mol. Finally, the zeolite proton interacts with the OH group which leads to formation of H_2O and $PhNN^+$ cation. This step requires overcoming of a very low barrier, 11 kJ/mol, and it is exothermic by 69 kJ/mol.

Furthermore, because we observed that NO^+ reaction with ammonia is not exclusive to zeolite and that inorganic nitrosyl salts (such as $NO[BF_4]$) react with ammonia to form molecular nitrogen at temperatures as low as -50 ºC, two pathways for the SCR reaction with ammonia on BF_4^-/NO^+ were investigated: (1) with and (2) without the direct participation of the boron fluoride complex (Figure 10, Table 1). Both schemes start with adsorption of ammonia to the BF_4^-/NO^+ substrate forming H_3NNO^+ species, as the binding energy is -91 kJ/mol. In the first step one of the H atoms of H_3NNO^+ moves to the BF_4^- anion. The reaction step is slightly endothermic by 15 kJ/mol and requires overcoming barrier of 16 kJ/mol. In

the final structure the nitrosamine and hydrogen fluoride are produced and bound by a hydrogen bond

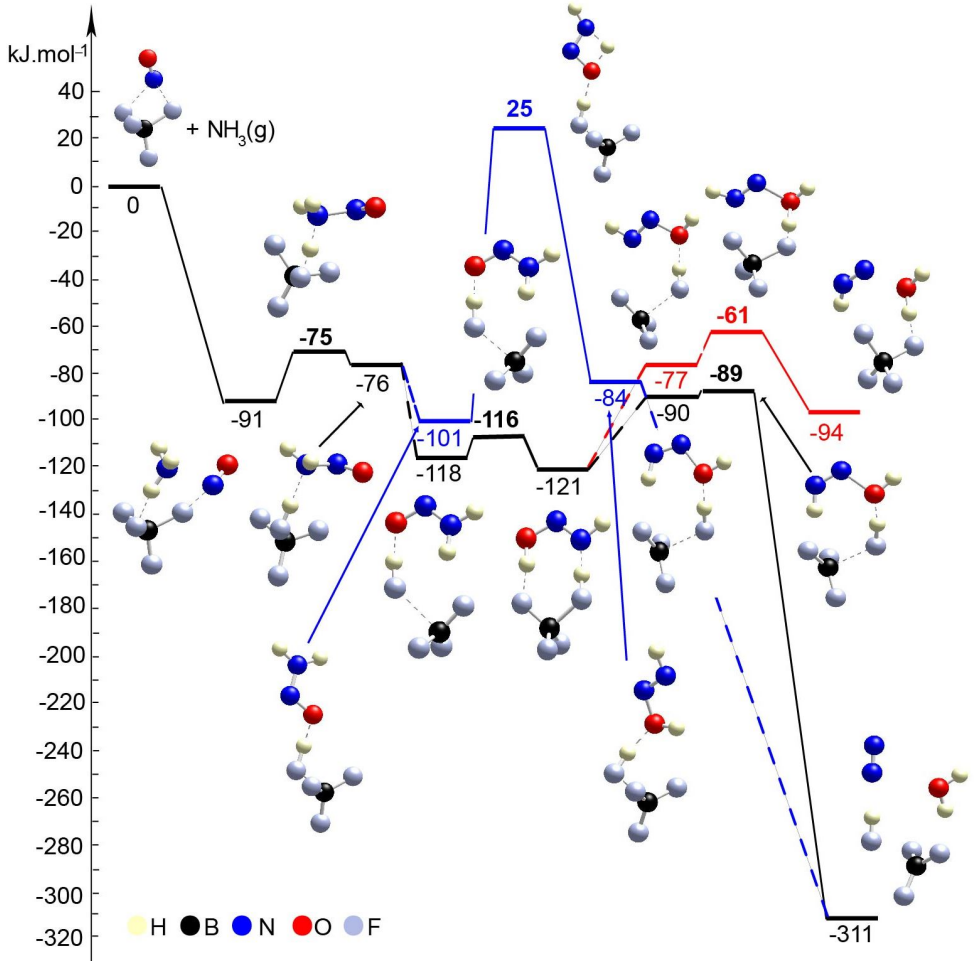

Figure 10. Energy diagram and optimized models of reaction steps for the interaction of BF_4/NO^+ with NH_3 (with and without direct participation of the BF_4^-). The models are visualized with VESTA program [34].

between H from the BF_3-HF complex and the N from the amino group. Further, a rearrangement of the complex occurs, so that the O atom interacts with the proton from BF_3-HF complex. This complex is more stable by 25 kJ/mol than the previous one, while if a second hydrogen bond is formed further stabilization of 17 kJ/mol is achieved. In the next step nitrosamine transforms into HN=NOH. This can be achieved without direct participation of the BF_3-HF substrate as one of the H atoms migrates from amino group to the O atom. This requires overcoming of a very high barrier, 126 kJ/mol, as the step is slightly endothermic, 17 kJ/mol. Alternatively, HN=NOH can be formed via synchronous transition state structure with the participation of BF_3-HF substrate. Synchronous the proton from HF migrates to the O center from nitrosamine molecule, while one of the H atoms from amino group migrates back to another F^- center. In

this way, the process is essentially barrierless and energetically neutral. Further, there are three possibilities for HN=NOH molecule to be transformed into N_2 and H_2O: (1) migration of H from NH to the O

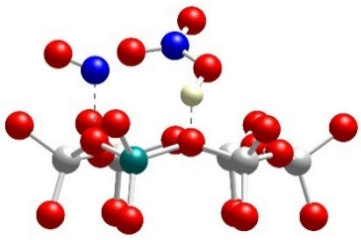

$ZEO/NO^+(HNO_3)$

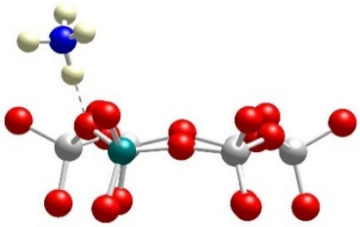

ZEO/NH_4^+

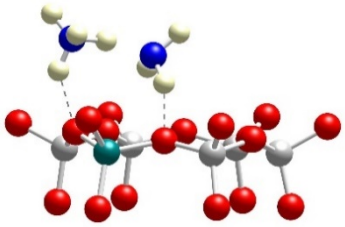

$ZEO/NH_4^+(NH_3)$

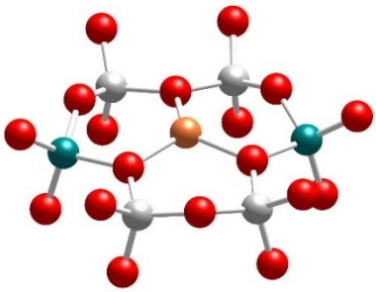

$ZEO(2Al\_6ring)/Cu^{2+}$

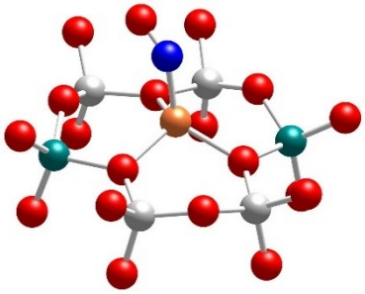

$ZEO(2Al\_6ring)/Cu^{2+}(NO)$

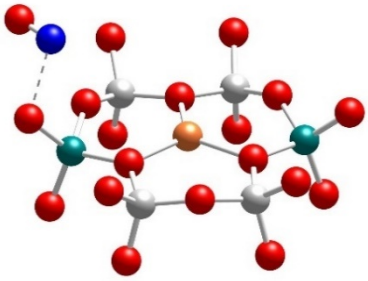

$ZEO(2Al\_6ring)/(Cu^+ + NO^+)$

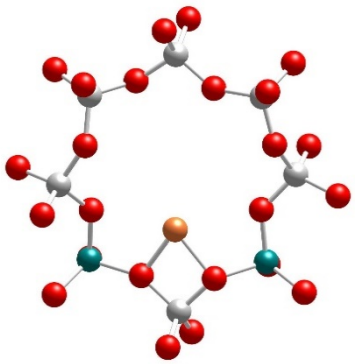

$ZEO(2Al\_8ring)/Cu^{2+}$

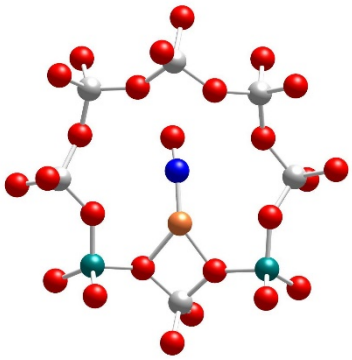

$ZEO(2Al\_8ring)/Cu^{2+}(NO)$

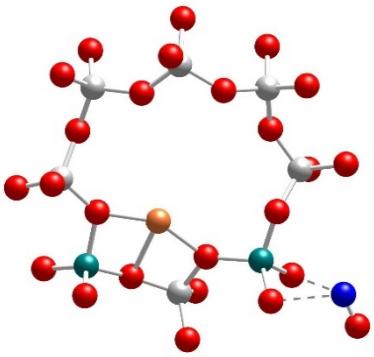

$ZEO(2Al\_8ring)/(Cu^+ + NO^+)$

Figure 11. Optimized structures of selected models. The models are visualized with VESTA program [34].

center without participation of the BF_3-HF complex (this way was not modeled since it is expected that such reaction step will occur with a very high barrier); (2) via synchronous transition state structure where H_2O and N_2 are formed in one step; (3) concerted mechanism where in the first step H_2O and NNH^+ are formed and afterwards N_2 is formed as the H^+ migrates to the BF_4^- moiety. The second concerted mechanism is most probable as it is essentially barrierless and strongly exothermic by 221 kJ/mol.

In order to assess the favorability of Cu(II) reduction by NO in SSZ-13, we considered the reduction of Cu^{2+} located in six and eight membered ring of CHA type zeolite structure containing two Al centers by NO (the structures are shown in Figure 11). First, we modeled formation of Cu^{2+}(NO) complex in the zeolite, which is exothermic by -145 and -203 kJ/mol, respectively. In the second step, the complex converts to two cationic species (Cu^+ and NO^+) each of them compensates one Al center. This step is endothermic by 31 and 43 kJ/mol. Thus, the overall exothermicity of the reduction of Cu^{2+} by NO to Cu^+ and NO^+ is -114 and -160 kJ/mol, respectively. This is fully consistent with our experimental findings.

$$\mathrm{ZEO(2Al\_6ring)/Cu^{2+}+NO(g)} \xrightarrow{\Delta E=-145\ \mathrm{kJ/mol}} \mathrm{ZEO(2Al\_6ring)/Cu^{2+}(NO)} \xrightarrow{\Delta E=31\ \mathrm{kJ/mol}} \mathrm{ZEO(2Al\_6ring)/(Cu^{+}+NO^{+})}$$

$$\mathrm{ZEO(2Al\_8ring)/Cu^{2+}+NO(g)} \xrightarrow{\Delta E=-203\ \mathrm{kJ/mol}} \mathrm{ZEO(2Al\_8ring)/Cu^{2+}(NO)} \xrightarrow{\Delta E=43\ \mathrm{kJ/mol}} \mathrm{ZEO(2Al\_8ring)/(Cu^{+}+NO^{+})}$$

Additionally, we modeled the steps regarding NO^+ formation and NH_3 adsorption in zeolite which are all highly favorable and exothermic. In agreement with earlier experimental studies for NH_3 adsorption, interaction of NH_4^+ ions with NH_3 is also very favorable [25].

1) $\mathrm{2\times NO(g)+\frac{1}{2}\times O_2(g)+2\times ZEO/H^+} \xrightarrow{\Delta E=-188\ \mathrm{kJ/mol}} \mathrm{2\times ZEO/NO^+ + H_2O(g)}$

2) $\mathrm{N_2O_4\,(g)+ZEO/H^+} \xrightarrow{\Delta E=-14\ \mathrm{kJ/mol}} \mathrm{ZEO/NO^+(HNO_3)} \xrightarrow{\Delta E=60\ \mathrm{kJ/mol}} \mathrm{ZEO/NO^+ + HNO_3(g)}$

3) $\mathrm{ZEO/H^+ + NH_3(g)} \xrightarrow{\Delta E=-166\ \mathrm{kJ/mol}} \mathrm{ZEO/NH_4^+}$

4) $\mathrm{ZEO/NH_4^+ + NH_3(g)} \xrightarrow{\Delta E=-90\ \mathrm{kJ/mol}} \mathrm{ZEO/NH_4^+(NH_3)}$

To summarize the DFT results, we investigated two pathways for the NO reduction reaction with ammonia on both substrates (zeolite/NO^+ and BF_4^-/NO^+): (1) with and (2) without the direct participation of the substrate. When the reaction occurs on the zeolite/NO^+ system with the participation of the zeolite (Figure 7) the barriers are very low (all of them are below 20 kJ/mol) manifesting that the reaction can occur at very low temperatures in line with our experimental results. However, if the zeolite does not participate

in the catalytic process directly, the barriers are >130 kJ/mol (Figure 8). According to our calculations, nitrosamine (NH_2NO) can be formed as an intermediate (see Figure 7), but the barrier for its transformation is very low. Similarly, NNH^+ species can be formed as well (Figure 7) which we prove experimentally through studies with phenyl diazonium cation (that is more stable than NNH^+ in Fig. 4). The results with the other substrate, BF_4^-/NO^+, are similar (Figure 10). When NH_3 is decomposed with the participation of the HF-BF_3 substrate the barriers are very low, while if the substrate does not participate in the reaction directly some of the barriers become higher than 120 kJ/mol. Similar results are also found for the aniline reduction (Figure 9), where $PhNN^+$ can be formed via the catalytic role of the zeolite as the highest barrier in the initial rate-limiting step is only 31 kJ/mol.

Based on these combined theoretical and experimental data, we can suggest that the role of copper is to promote NO^+ formation since Brønsted acid sites get occupied by NH_4^+ after NO^+ reacts with NH_3 on bare H-Zeolite and they cannot contribute to NO^+ formation as we showed herein. The resulting NO^+ reacts with ammonia to reform N_2. The $Cu(I)(NH_3)_2$ complex, in turn, gets re-oxidized back to Cu(II) with oxygen [17,18]. Notably, this bears striking resemblance to the recent advances in enzymatic chemistry on Cu-containing enzymes for denitrification and annamox (anaerobic ammonia oxidation to nitrogen) processes. Only in recent decades, pioneering studies of Murphy and co-workers (for denitrification) [32], and Kartal, Strous, and co-workers (for annamox) [33] reactions revealed the central role of Cu(I)---NO^+ intermediate and diazo-compounds for these processes. Our data point to the presence of the similar active site for Cu-zeolite system (used industrially in vehicles) and Cu-enzymes, occurring in nature.

We note that our findings represent the first observation of the potential intermediates of NO reduction with ammonia (SCR) responsible for N-N bond formation for zeolites and copper-zeolite systems and lay out the strategy to investigate vehicle-relevant SCR under more complex gas feeds (that include water and hydrocarbons, in addition to oxygen, NO and ammonia): under these complex vehicle-relevant gas conditions additional mechanistic pathways, leading to N-N coupling, may also be operative.

Acknowledgments

IZK is thankful to the financial support received from the program "Young scientists and Postdoctoral candidates" of the Bulgarian Ministry of Education and Science, MCD № 95/20.12.2019. HAA and GNV acknowledge the support of the project EXTREME, funded by the Bulgarian Ministry of Education and Science, D01-76/30.03.2021 through the programme “European Scientific Networks”.

The research at PNNL was supported by the U.S. Department of Energy, Energy Efficiency and Renewable Energy, Vehicle Technology Office. Experiments were conducted in the Environmental Molecular

Sciences Laboratory (EMSL), a national scientific user facility sponsored by the Department of Energy's Office of Biological and Environmental Research at Pacific Northwest National Laboratory (PNNL). PNNL is a multi-program national laboratory operated for the DOE by Battelle Memorial Institute under Contract DE-AC06-76RL01830. We acknowledge the support of CLEERS (Crosscut Lean Exhaust Emissions Reduction Simulations). CLEERS is an initiative funded by the U.S. Department of Energy (DOE) Vehicle Technologies Office to support the development of accurate tools for use in the design, calibration, and control of next generation engine/emissions control systems that maximize efficiency while complying with emissions regulations.

References

(1) Royal College of Paediatrics and Child Health . Every breath we take—the lifelong impact of air pollution. London: Royal College of Paediatrics and Child Health, 2016.
(2) W.M.H. Sachtler, Catalysis from Art to Science. In: Carley A.F., Davies P.R., Hutchings G.J., Spencer M.S. (eds) Surface Chemistry and Catalysis. Fundamental and Applied Catalysis. Springer, Boston, MA, 2002.
(3) M. K. Khair, W. A. Majewski, Diesel emissions and their control; SAE International, Warrendale, 2006.
(4) T. Seiyama, T. Arakawa, T. Matsuda, N. Yamazoe, Y. Takita, Catalytic reduction of nitric oxide with ammonia over transition metal ion-exchanged zeolites, Chem. Lett. 1975, 781.
(5) S. I. Zones, Zeolite SSZ-13 and its method of preparation, US Pat 4 544 538, 1985.
(6) J.-H. Kwak, R. G. Tonkyn, D. H. Kim, J. Szanyi, C. H. Peden, Excellent activity and selectivity of Cu-SSZ-13 in the selective catalytic reduction of NOx with NH_3, J. Catal. 2010, 275, 187-190.
(7) I. Bull, A. Moini, G. Koermer, J. Patchett, W. Jaglowski, S. Roth, Zeolite catalyst with improved NOx reduction in SCR, US Patent US20070134146A1, 2010.
(8) D. W. Fickel, R. F. Lobo, Copper Coordination in Cu-SSZ-13 and Cu-SSZ-16 Investigated by Variable-Temperature XRD, J. Phys. Chem. C 2010, 114, 1633-1640.
(9) J.H. Kwak, D. Tran, S.D. Burton, J. Szanyi, J.H. Lee, C.H.F. Peden, Effects of hydrothermal aging on NH3-SCR reaction over Cu/zeolites, J. Catal. 2012, 203.
(10) J.H. Kwak, D. Tran, J. Szanyi, C.H.F. Peden, J.H. Lee, The Effect of Copper Loading on the Selective Catalytic Reduction of Nitric Oxide by Ammonia Over Cu-SSZ-13, Catal. Lett. 2012, 142, 295.
(11) S.J. Schmieg, S.H. Oh, C.H. Kim, D.B. Brown, J.H. Lee, C.H.F. Peden, D.H. Kim, Thermal durability of Cu-CHA NH3-SCR catalysts for diesel NOx reduction, Catal. Today 2012, 184, 252.
(12) J.H. Kwak, H.Y. Zhu, J.H. Lee, C.H.F. Peden, J. Szanyi, Two different cationic positions in Cu-SSZ-13? Chem. Commun. 2012, 48, 4758.
(13) F. Gao, J. H. Kwak, J. Szanyi and C. H. F. Peden, Current Understanding of Cu-Exchanged Chabazite Molecular
(14) Sieves for Use as Commercial Diesel Engine DeNOx Catalysts, Top. Catal. 2013, 56, 1441–1459.
(15) S. T. Korhonen, D.W. Fickel, R.F. Lobo, B.M. Weckhuysen, A.M. Beale, Isolated Cu^{2+} ions: active sites for selective catalytic reduction of NO, Chem. Comm. 2010, 47, 800-802
(16) F. Gao, E. D. Walter, E. M. Karp, J. Y. Luo, R. G. Tonkyn, J. H. Kwak, J. Szanyi and C. H. F. Peden, Synthesis and Evaluation of Cu-SAPO-34 Catalysts for Ammonia Selective Catalytic Reduction. 1. Aqueous Solution Ion Exchange, J. Catal. 2013, 300, 20–29.
(17) J. H. Kwak, T. Varga, C. H. F. Peden, F. Gao, J. C. Hanson, J. Szanyi, Following the movement of Cu ions in a SSZ-13 zeolite during dehydration, reduction and adsorption: A combined in situ TP-XRD, XANES/DRIFTS study, J. Catal., 2014, 314, 83–93.
(18) F. Gao, D. Mei, Y. Wang, J. Szanyi, C.H.F. Peden, Selective Catalytic Reduction over Cu/SSZ-13: Linking Homo- and Heterogeneous Catalysis, J. Am. Chem. Soc. 2017, 139, 4935−4942.
(19) F. Gao, E. D. Walter, M. Kollar, Y. Wang, J. Szanyi, C.H.F. Peden, Understanding ammonia selective catalytic reduction kinetics over Cu/SSZ-13 from motion of the Cu ions, J. Catal. 2014, 319, 1−14.
(20) A. M. Beale, F. Gao, I. Lezcano-Gonzalez, C.H.F. Peden, J. Szanyi, Recent advances in automotive catalysis for NOx emission control by small-pore microporous materials, J. Chem. Soc. Rev. 2015, 44, 7371−7405.
(21) J. H. Kwak, J. H. Lee, S. D. Burton, A. S. Lipton, C. H. F. Peden, J. Szanyi, A common intermediate for N2 formation in enzymes and zeolites: side-on Cu-nitrosyl complexes, Angew. Chem. Int. Ed. 2013, 52, 9985–9989.

(22) K. I. Hadjiivanov, Identification of Neutral and Charged NxOy Surface Species by IR Spectroscopy, Catal. Rev. Sci. Eng. 2000, 42, 71-144.
(23) K. Hadjiivanov, J. Saussey, J. L. Freysz, J. C. Lavalley, FT-IR study of NO + O2 co-adsorption on H-ZSM-5: re-assignment of the 2133 cm^{-1} band to NO^{+} species, Catal. Lett. 1998, 52, 103–108.
(24) J. Szanyi, M. T. Paffett, The Adsorption of NO and Reaction of NO with O2on H-, NaH-, CuH-, and Cu-ZSM-5: Anin SituFTIR Investigation, J. Catal. 1996, 164, 232–245.
(25) A. Zecchina, L. Marchese, S. Bordiga, C. Paze, E. Gianotti, Vibrational Spectroscopy of NH_4^{+} Ions in Zeolitic Materials: An IR Study, J. Phys. Chem. B 1997, 101, 10128.
(26) C. Negri, T. Selleri, E. Borfecchia, A. Martini, K. A. Lomachenko, T. V. W. Janssens, M. Cutini, S. Bordiga, G. Berlier, G. Structure and Reactivity of Oxygen-Bridged Diamino Dicopper(II) Complexes in Cu-Ion-Exchanged Chabazite Catalyst for NH_3-Mediated Selective Catalytic Reduction, J. Am. Chem. Soc. 2020, 142, 15884−15896.
(27) K. Chakarova, K. Hadjiivanov, H-Bonding of Zeolite Hydroxyls with Weak Bases: FTIR Study of CO and N_2 Adsorption on H-D-ZSM-5, J. Phys. Chem. C 2011, 115, 4806.
(28) D. Perra, N. Drenchev, K. Chakarova, M.G. Cutrufello, K. Hadjiivanov, Remarkable acid strength of ammonium ions in zeolites: FTIR study of low-temperature CO adsorption on NH_4-FER, RSC Adv. 2014, 4, 56183-56187.
(29) L. A. Kazitsyna, B. S. Kikot, O. A. Reutov, Infrared absorption spectra of solutions of diazonium salts in the region of 2200–2300 cm^{-1}, Bull. Acad. Sci. USSR, Div. Chem. Sci. (Engl. Transl.) 1964, 13, 894.
(30) J. Szanyi, J.H. Kwak, C.H.F. Peden, The Effect of Water on the Adsorption of NO_2 in Na− and Ba−Y, FAU Zeolites: A Combined FTIR and TPD Investigation, J. Phys. Chem. B 2012, 108 (12), 3746-3753.
(31) K. Khivantsev, N. R. Jaegers, I. Z. Koleva, H. A. Aleksandrov, L. Kovarik, M. Engelhard, F. Gao, Y. Wang, G. N. Vayssilov, J. Szanyi, Stabilization of Super Electrophilic Pd+2 Cations in Small-Pore SSZ-13 Zeolite, J. Phys. Chem. C 2020, 124, 309–321.
(32) E. I. Tocheva, F. I. Rosell, G. Mauk, M. E. P. Murphy, Side-on copper-nitrosyl coordination by nitrite reductase, Science 2004, 7, 867-870.
(33) B. Kartal, W. J Maalcke, N. M de Almeida, I. Cirpus, J. Gloerich, W. Geerts, H. J M Op den Camp, H. R, Harhangi, E. M. Janssen-Megens, K.-J. Francoijs, H. G Stunnenberg, J. T Keltjens, M. S M Jetten, M. Strous, Molecular mechanism of anaerobic ammonium oxidation, Nature 2011, 479, 127-130.
(34) K. Momma, F. Izumi, "VESTA 3 for three-dimensional visualization of crystal, volumetric and morphology data," J. Appl. Crystallogr. 2011, 44, 1272-1276.

Competing interests: Authors have no conflicts to declare.

Supporting Information:

Identification of the mechanism of NO reduction with ammonia (SCR) on zeolite catalysts

Authors: Konstantin Khivantsev[1*]†, Ja-Hun Kwak[2*]†, Nicholas R. Jaegers[1*], Iskra Z. Koleva[3]†, Georgi. N. Vayssilov[3], Miroslaw A. Derewinski[1,4], Yong Wang[1], Hristiyan A. Aleksandrov[3*]† and Janos Szanyi[1*]†

Affiliations:

[1]Pacific Northwest National Laboratory Richland, WA 99352 USA

[2] Ulsan National Institute of Science and Technology (UNIST), South Korea

[3]Faculty of Chemistry and Pharmacy, University of Sofia, 1126 Sofia, Bulgaria

[4] J. Haber Institute of Catalysis and Surface Chemistry, Polish Academy of Sciences, Krakow 30-239, Poland

* Correspondence to: K.K, JHK, NRJ, HAA, J.Sz.

† These authors contributed equally to the manuscript

Materials and methods

BEA with Si/Al ratio ~ 15 was synthesized in the presence of fluoride anions according to a procedure developed by Camblor et al. [S1] The gel composition was as follows SiO_2: xAl_2O_3:(0.54 + 2x)TEAOH:(0.54 + 2x)HF:(7 + 2x)H_2O. The absence of alkali cations requires only a calcination step (550 ºC in flowing air), decomposing the organic cation (TEA^+) to convert it into Brønsted acidic H-Form.

Na/SSZ-13 zeolite with Si/Al 12 was hydrothermally synthesized using the following recipe: 0.8 g of NaOH (Sigma Aldrich, ≥ 99%) was dissolved in 50 ml of deionized water. 17 g of TMAda-OH (Sachem Inc., 25% N,N,N-trimethyl-1-adamantyl ammonium hydroxide) was added as structure directing agent. 0.75 g of $Al(OH)_3$ (Sigma Aldrich, ~54% Al_2O_3) was slowly added to the solution and stirred at 400 rpm until it was completely dissolved. 20.0 g of LUDOX HS-30 colloidal silica (Sigma Aldrich, 30 wt% suspension in H_2O) was added slowly to the solution until a uniform gel was formed. The obtained gel was sealed in a 125 mL Teflon-lined stainless steel autoclave with a magnetic stirring bar. Hydrothermal synthesis was carried out at 160 °C under continuous stirring at 400 rpm for 4 days. After synthesis, the zeolite cake was separated from the suspension by centrifugation, and washed with deionized water. It was then dried at 80 °C under N_2 flow overnight, and calcined in air at 550 °C for 5 h in order to remove the SDA. NH_4/SSZ-13 was obtained by ion exchange of the as-prepared Na/SSZ-13 zeolite with 1 M NH_4NO_3 solution at 80 °C for 5 h. The process was

repeated three times. H-form of zeolite was obtained by calcining in air at 550 ºC for 5 hours. Ion-exchange with Cu(II) to produce Cu/SSZ-13 was performed in the presence of copper nitrate. The resulting sample was calcined at 550 ºC in air.

$NO[BF_4]$ nitrosyl tetrafluoroborate (99%) was purchased from Strem Chemicals and stored cold in the absence of moisture.

All the chemicals used were the highest-grade purity available.

HAADF-STEM analysis was performed with a FEI Titan 80–300 microscope operated at 300 kV. The instrument is equipped with a CEOS GmbH double-hexapole aberration corrector for the probe-forming lens, which allows for imaging with 0.1 nm resolution in scanning transmission electron microscopy mode (STEM). The images were acquired with a high angle annular dark field (HAADF) detector with inner collection angle set to 52 mrad.

Helium ion microscopy (HIM) images were obtained using 35 keV He ions with 0.1 pA beam current at normal incidence. Secondary electrons were detected using an Everhart–Thornley detector. For HIM imaging, a very thin layer of carbon (<1 nm) was coated using a carbon sputter deposition system as the samples were completely insulating. The instrument resolution was 0.35 nm.

The *in-situ* static transmission IR experiments were conducted in a home-built cell housed in the sample compartment of a Bruker Vertex 80 spectrometer, equipped with an MCT detector and operated at 4 cm^{-1} resolution. The powder sample was pressed onto a tungsten mesh, which, in turn, was mounted onto a copper heating assembly attached to a ceramic feedthrough. The sample could be resistively heated, and the sample temperature was monitored by a thermocouple spot welded onto the top center of the W grid. The cold finger on the glass bulb containing CO (99.995%) was cooled with liquid nitrogen to eliminate any contamination originating from metal carbonyls, while NO (99.95%) was cleaned with multiple freeze–pump–thaw cycles. $^{15}NH_3$ (15N, 98%) was purchased from Cambridge Isotopes. Special research-grade oxygen (purity 99.995%) was purchased from Oxarc.

The NO reduction by ammonia (in the presence of oxygen) was carried out in a typical quartz tube plug-flow reactor. 120 mg of H-zeolites was used for reaction tests. The composition of the gas flowing through the catalyst was ~360 ppm NH_3, 360 ppm NO, ~12 % O_2 balanced with nitrogen. The total flow rate was ~ 300 sscm/min. Concentrations of reactants and products were measured by the FTIR analyzer.

Computational details

We performed periodic DFT calculations with VASP program [S2] using PBE functional [S3] with empirical correction D2 for the dispersion interactions [S4], as well as PAW pseudopotentials S5]. The cut-off energy was set to 700 eV. The *Brillouin zone was sampled* only using the Gamma point only. For the geometry optimization, the threshold for the relaxation of the forces acting on each atom is 0.1 $eV/Å^2$. The chabazite model contains in total 108 atoms per unit cell (36 T atoms and 72 O atoms) with the following dimensions: a = b = 13.675 Å, c = 14.767 Å; α = β = 90°, γ = 120°. To create negative charge in the zeolite framework one or two Si are substituted with Al. The general location of the species sorbed in the pores of the periodic chabazite model is presented in Figure 7A.

The energies of the reactions are calculated as follows: $\Delta E = E_P - E_R$, where the E_p is the total energy of the products and E_R is the total energy of the reactants. Thus, negative value of ΔE indicates that the reaction is energetically favorable. In the same way, the activation barriers are calculated as the difference between the energies of the transition state and the initial state (reactants).

References

S1 M.A. Camblor, A. Corma, S. Valencia Synthesis in fluoride media and characterisation of aluminosilicate zeolite beta, J. Mater. Chem., 8 (1998), pp. 2137-2145

S2 G. Kresse, J. Furthmüller, Comput. Mater. Sci. 1996, 6, 15.
S3 J. P. Perdew, K. Burke, M. Ernzerhof, Phys. Rev. Lett. 1996, 77, 3865.
S4 S. Grimme. J. Comput. Chem. 2006, 27, 1787−1799.
S5 P. E. Blöchl, Phys. Rev. B, 1994, 50, 17953.

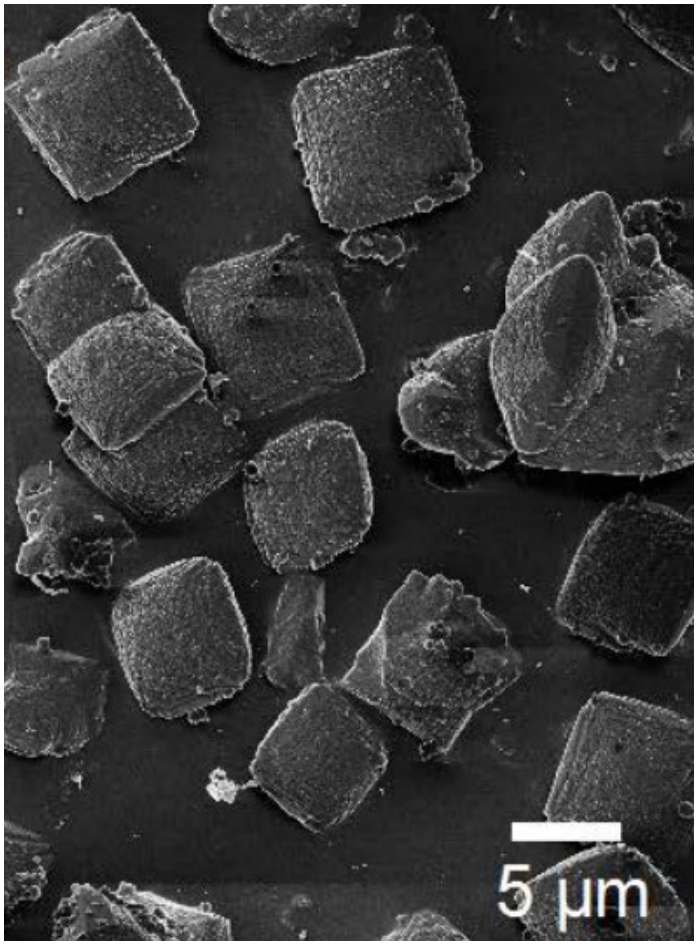

Figure S0. Typical Helium Ion Microscopy (HIM) image of H-BEA crystals with Si/Al ~ 15.

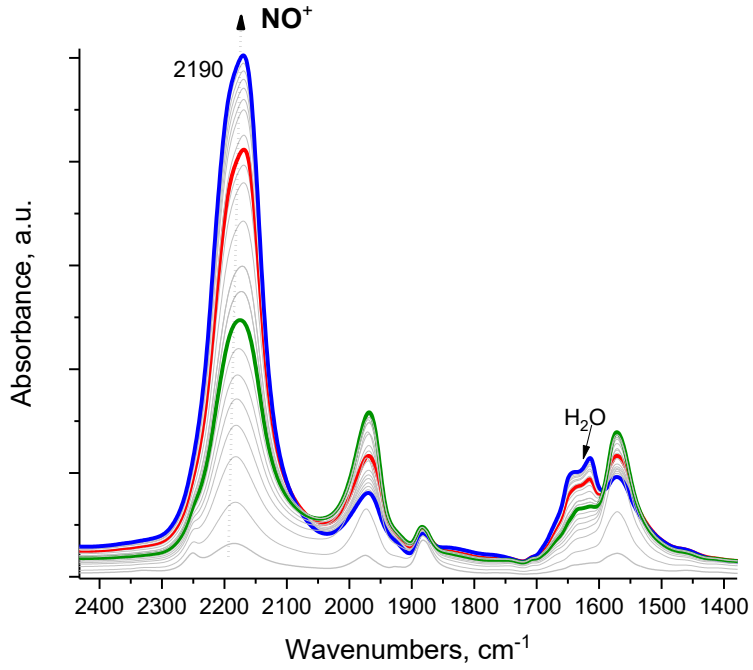

Figure S1. *In-situ* FTIR during sequential NO (0.5 Torr) and O_2 (0.1 Torr) co-adsorption on H-SSZ-13 with Si/Al~12 at room temperature.

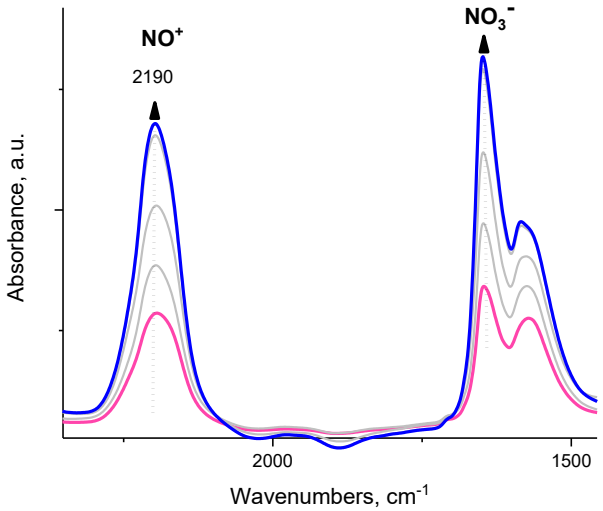

Figure S2. *In-situ* FTIR during sequential NO_2 (0.5 Torr) on H-SSZ-13 with Si/Al~12 at room temperature. NO_2 forms N_2O_4 in the pores and immediately reacts with H-SSZ-13 to form NO^+ and HNO_3.

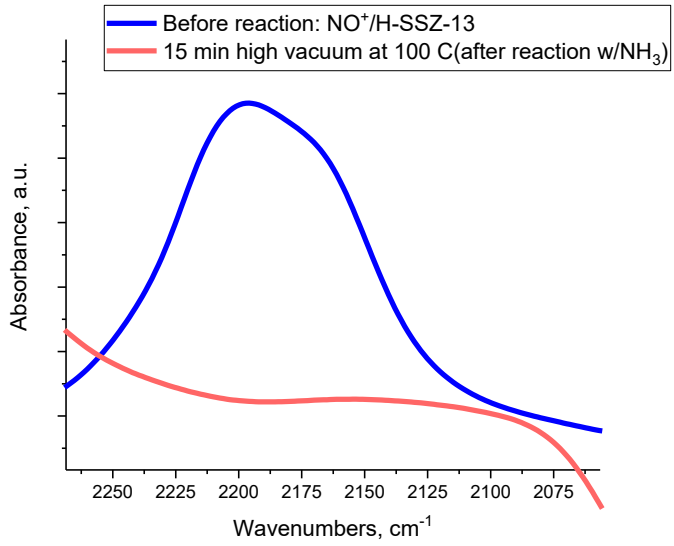

Figure S3. *Continuing from Fig 5 in the Main Text.* FTIR of the N-O stretching region of NO+/H-SSZ-13 system before reaction with ammonia, and after reaction with ammonia (at room temperature), and after pulling high vacuum at 100 ºC for 15 minutes.

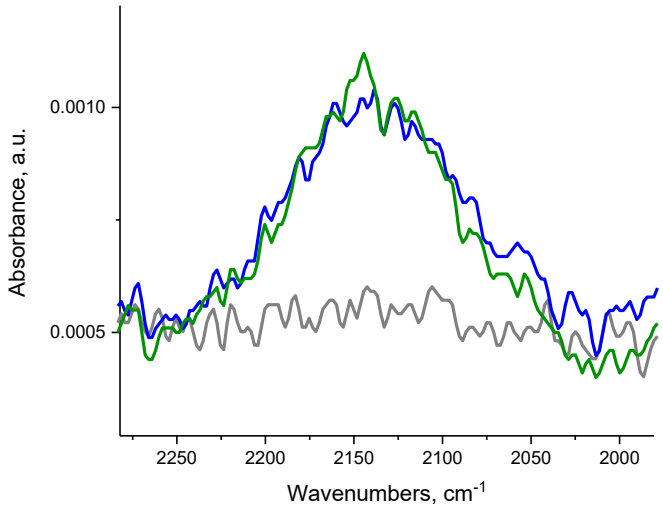

Figs. S4. *Continuing FTIR experiments after the ones performed in Fig 2A.* After reaction between NO^+/H-BEA with $^{15}NH_3$, the sample was vacuumed at room temperature and new baseline was collected (gray spectrum). 2 Torr NO + 0.7 Torr O_2 were then reacted with the sample: the resulting spectra (green and blue) show that because NH_3 occupied Brønsted acid sites of zeolite with the formation of NH_4-Zeolite (ammonia is strongly adsorbed and cannot be desorbed at room temperature even to a small extent), only extremely small amounts of NO_2 can be formed (intensities barely above the noise level).

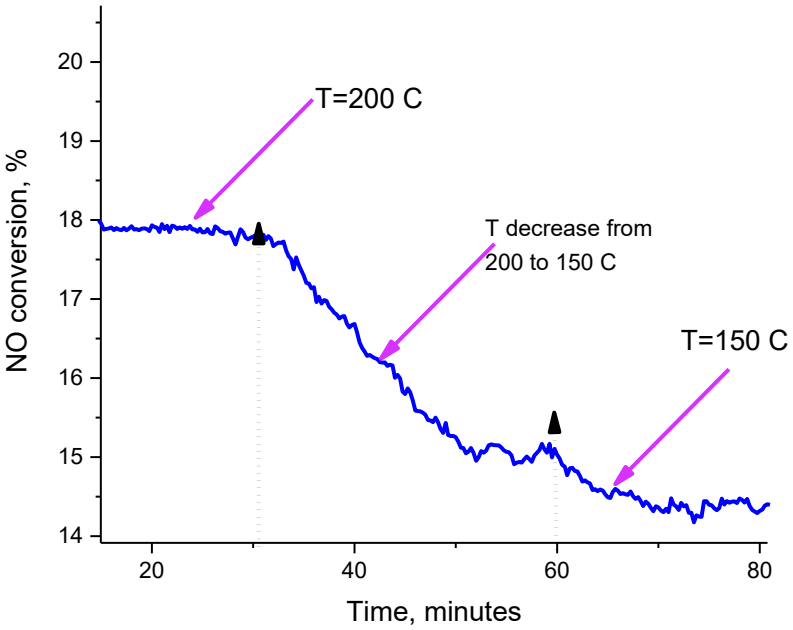

Figs. S5. NO conversion (%) vs time-on-stream for H-BEA Si/Al ~ 15 sample under dry conditions (conditions specified in experimental section).

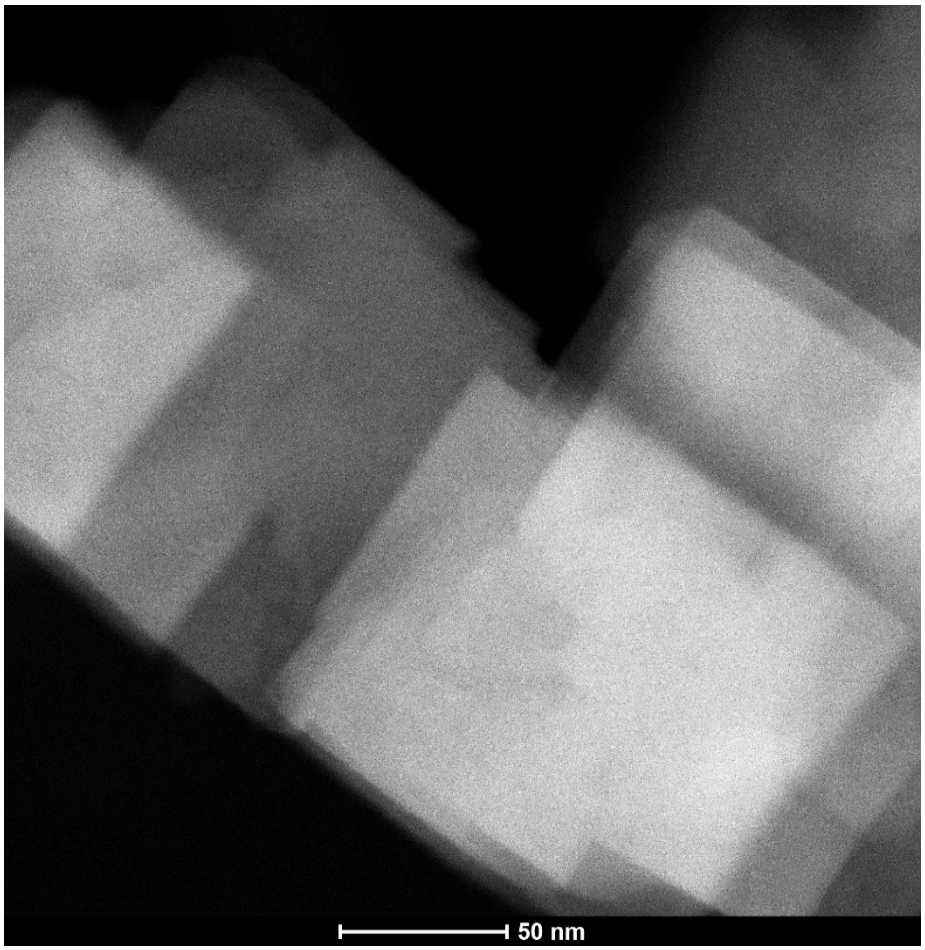

Figure S6. Typical HAADF-STEM images of SSZ-13 crystals.